HAL
open science

A method to generate near real time UV-Index maps of Austria

B. Schallhart, M. Blumthaler, J. Schreder, J. Verdebout

To cite this version:

B. Schallhart, M. Blumthaler, J. Schreder, J. Verdebout. A method to generate near real time UV-Index maps of Austria. Atmospheric Chemistry and Physics Discussions, 2008, 8 (1), pp.2143-2161. hal-00303284

HAL Id: hal-00303284

https://hal.science/hal-00303284v1

Submitted on 18 Jun 2008

HAL is a multi-disciplinary open access archive for the deposit and dissemination of scientific research documents, whether they are published or not. The documents may come from teaching and research institutions in France or abroad, or from public or private research centers.

L'archive ouverte pluridisciplinaire **HAL**, est destinée au dépôt et à la diffusion de documents scientifiques de niveau recherche, publiés ou non, émanant des établissements d'enseignement et de recherche français ou étrangers, des laboratoires publics ou privés.

Atmos. Chem. Phys. Discuss., 8, 2143–2161, 2008
www.atmos-chem-phys-discuss.net/8/2143/2008/
© Author(s) 2008. This work is distributed under
the Creative Commons Attribution 3.0 License.

Atmospheric Chemistry and Physics Discussions

A method to generate near real time UV-Index maps of Austria

B. Schallhart[1], M. Blumthaler[1], J. Schreder[2], and J. Verdebout[3]

[1]Division of Biomedical Physics, Innsbruck Medical University, Muellerstrasse 44, 6020 Innsbruck, Austria
[2]CMS Ing.Dr.Schreder GmbH, Eggerstrasse 8, 6322 Kirchbichl, Austria
[3]European Commission, Joint Research Centre, Institute for Health and Consumer Protection, Via E. Fermi 1, 21020 Ispra (VA), Italy

Received: 20 December 2007 – Accepted: 20 December 2007 – Published: 6 February 2008

Correspondence to: B. Schallhart (barbara.schallhart@i-med.ac.at)

Published by Copernicus Publications on behalf of the European Geosciences Union.

Abstract

A method is presented that combines individual ground based ultraviolet (UV) measurements from the Austrian UVB monitoring network and area-wide data of the distribution of clouds derived from satellite images to generate a UV-Index map all over the region. The Austrian UVB Monitoring network provides near real time ground based measurements of surface UV irradiance from fifteen selected locations throughout and in the vicinity of Austria. The amount of ultraviolet radiation passing through the atmosphere as measured by the UVB detectors is indicated in units of the UV-Index, the internationally agreed unit for erythemally weighted solar UV irradiance. Together with clear sky model calculations the measured UV-Index is used to determine the cloud modification factor (CMF), a scaling factor giving the reduction of radiation due to the presence of clouds. Moreover satellite images from MSG (Meteosat Second Generation) with a time resolution of 15 min and a spatial resolution of 0.05° are received. From the satellite images the CMFs for the area of Austria are obtained using an algorithm provided by Jean Verdebout. Then both independent data sets of cloud modification factors are checked for consistency by comparing satellite derived and ground based values at the positions of the monitoring stations. If necessary the satellite derived cloud modification factors are corrected by about ±20% according to the results of the ground based measurements. Afterwards realistic UV-Index maps of the whole area are generated by scaling model derived UV-Indexes with the corresponding cloud modification factors. Since all the data is available in almost real time, the calculated UV-Index maps are available in the web at http://www.uv-index.at/ with a time delay of about 30 min.

1 Introduction

Since the discovery of the Antarctic ozone hole in 1985 several studies of stratospheric ozone depletion have been performed showing that this phenomenon is not only con-

fined to the Antarctic continent. This fact led to concerns about increasing UV radiation at the earth's surface and motivated more profound investigations in measuring and modelling UV radiation. A lot of countries including Austria established monitoring networks to quantify the amount of UV radiation at the ground with high accuracy. At the present time the Austrian UVB monitoring network consists of fifteen ground based detectors in selected locations. Since the main climatological parameters influencing UV radiation like clouds, ozone and aerosols vary on a small scale depending on geographical conditions and wind situation, it is difficult to extend the localized UV measurements to a broader scale without additional information. Although ground based UV detectors are the reference in terms of accuracy they only offer information of the incident solar radiation in single spots. A method to obtain radiation maps based on ground measurements only is to interpolate spatially between the single point measurements. By using the Kriging method (Krige, 1981) together with elevation maps and long term correlations between the measurements, simple radiation maps are obtained (Schmalwieser and Schauberger, 2001). A shortcoming of this method is that effects of changing clouds on the surface radiation can not be taken into account.

On the other hand satellite images provide area-wide information of the atmosphere and the surface. So methods have been developed to map the surface UV radiation by combining modelling and satellite data (Verdebout, 2000). Surface UV radiation maps of Greece generated by this method can be found at http://lap.physics.auth.gr/uvnet.gr/. A disadvantage of satellite data is due to the dependency of the accuracy on the pixel resolution. Regional variations of the atmosphere and changes in the surface are smoothed over some square kilometres.

Here we present a method that uses a combination of ground based measurements as well as satellite derived data to calculate an area-wide UV-Index map of Austria. On one hand this method benefits from high accuracy of ground measurements and on the other hand from high geographical coverage of the satellite data.

2 Data from satellite and ground based measurements

The algorithm is based on two independent data sets that are satellite images from MSG taken at three spectral channels in the visible and infrared and ground based measurements of UV radiation gathered by the Austrian UVB monitoring network.

2.1 Satellite images from MSG

Since April 2005 so-called High Rate SEVIRI Image Data (EUMETSAT, 2005) is collected. This data is measured with the SEVIRI (Spinning Enhanced Visible and Infra-Red Imager) radiometer onboard the satellites of the Meteosat Second Generation series operated by the European Organisation for the Exploitation of Meteorological Satellites (EUMETSAT). On a 15 min basis images of the full disk of the earth are received in eleven spectral channels. The spatial resolution of the subsatellite point is 3×3 km, in the region of Austria the pixel size is approximately 5.5×4 km (north-south × east-west) which corresponds to a resolution of 0.05°. For further analysis only images at 600 nm, 1.6 µm and 12 µm are used.

2.2 The Austrian UVB monitoring network

The Austrian UVB monitoring network is operational since 1997 and consists of ten primary stations that are equipped with broadband UV-Biometers (Model 501 from Solar Light Co. Inc.) for measuring erythemally weighted solar UV irradiance. At the present time data from additional five measurement stations with broadband detectors is received to improve the geographical coverage thereby improving the quality of the generated UV-Index map. Within the area of Austria twelve stations are distributed in order to cover the most populated areas as well as different levels of altitude, see Table 1. In addition two detectors situated in Germany nearby the Austrian border at München and at Zugspitze as well as one station located at Davos (Switzerland) contribute to the network. The location of all stations within the UV-Index map can be seen

in Fig. 4.

International intercomparisons of broadband detectors (Leszczynski et al. (1998) and Bais et al. (2000)) have shown that there is a great variability between results from different instruments. Moreover the same detector may change from year to year by ±10%. Therefore the detectors are calibrated once a year by determining the spectral sensitivity in the laboratory. The absolute calibration is carried out by comparing solar broadband measurements to simultaneous measurements of a well-calibrated spectroradiometer. The uncertainty of the calibration is about ±7% (Blumthaler, 2004). In addition quality control is permanently done by comparing the measurements to clear sky calculations carried out with the model FastRT (Engelsen and Kylling, 2005).

The UV measurements are recorded as mean values over 10 or 30 min. Afterwards the raw data is sent to Innsbruck. To obtain absolute values the raw data is multiplied by a calibration function that is dependent on solar zenith angle and ozone. Finally the results are transferred in units of the UV-Index. The UV-Index is defined by the World Health Organization (WHO, 2002) as the measured solar global irradiance (in $mW\,m^{-2}\,nm^{-1}$) weighted with the erythemal action spectrum of the human skin, integrated from 250 up to 400 nm and finally divided by $25\,mW\,m^{-2}$. This leads to a dimensionless positive number that is ranging for most conditions in Europe from 0 to 10. Moreover at the high mountain station Sonnblick also the ozone column is measured daily by a Brewer spectroradiometer. This data is available at the following day. In order to calculate a clear sky UV prognosis of the current day ozone forecast data from DWD (Deutscher Wetter Dienst, German Weather Service) is used. Since one aim of the Austrian UVB Monitoring network is to increase the awareness of possible health risks induced by long-term exposure to solar UV radiation, all measurements and derived results including the UV-Index map are open to the public at http://www.uv-index.at/.

3 Method

First of all the two independent data sets are checked for consistency. Therefore satellite images as well as ground based measurements are evaluated in terms of cloud modification factors by using different algorithms. The cloud modification factor F is defined as a scaling factor giving the reduction of the clear sky UV-Index I_{clear} due to the presence of clouds, see Eq. (1)

$$I_{cloudy} = I_{clear} \times F \tag{1}$$

where I_{cloudy} is the reduced UV-Index due to clouds and $F=0...1$. So the lower limit of the cloud modification factor $F=0$ describes a totally overcast sky where no radiation is passing through the cloud field, whereas $F=1$ means that there are no clouds at all (clear sky).

3.1 Cloud modification factors from satellite images

For the determination of cloud modification factors from MSG satellite images an algorithm proposed by Verdebout (2000) is employed with some modifications. The original algorithm is used to calculate surface UV radiation maps based on METEOSAT data obtained with the MVIRI (Meteosat Visible and Infra-Red Imager) instrument, which is the precursor of the SEVIRI radiometer used nowadays. From this images together with snow cover data and a digital elevation model, the cloud liquid water thickness is derived. Based on this parameter and visibility observations and total column ozone from GOME satellite, interpolation in a UV lookup table leads to surface UV radiation maps. The whole algorithm is described in detail in Verdebout (2000). It was used to derive a surface UV radiation climatology for the period of 1984 up to 2003 that was tested against long-time ground based measurements performed at Ispra and in Thessaloniki (Verdebout, 2004). The comparison between satellite estimates and ground based measurements was conducted on daily doses to overcome some of the discrepancies that are inherent in the two different methods of data gathering. Satellite data

only provide averages over a certain area (the pixel size) whereas ground based measurements are sensitive to the detailed cloud structure. Also there are differences in the time averaging. In Ispra the rms value of the relative difference between the satellite estimates and the measured erythemal daily doses was found to be 29% and the bias was +3% ((satellite-ground)/ground). By comparing monthly doses the rms of the relative difference decreased to 5%. Similar results have been found for the comparison with Thessaloniki data and at four other European sites (Arola et al., 2002). Moreover the algorithm is known to have difficulties in distinguishing between high cirrus clouds and snow covered terrain from the three spectral satellite images. Especially in the area of the Austrian Alps this leads to discrepancies between satellite estimates and ground based measurements as described in Sect. 3.3.

In 2002 the launch of the first satellite of the MSG series took place. Since then advanced instrumentation like the SEVIRI radiometer is used to monitor the weather. So the algorithm had to be adapted to the new data specifications (Verdebout and Gröbner, 2004). Moreover the algorithm was modified for our purpose and a new parameter, the cloud modification factor, was implemented. The cloud modification factor F_{MSG} as defined in Eq. (1) is derived from the cloud optical thickness for each pixel (size $0.05^\circ \times 0.05^\circ$). An example of a satellite derived cloud modification factor map is given in Fig. 3.

3.2 Cloud modification factors from ground based measurements

In order to obtain cloud modification factors for each site of the Austrian UVB monitoring network the measured UV-Indexes I have to be compared to site specific clear sky model calculations $\tilde{I}$ of the UV-Index. Then the CMF for each site F_{ground} is obtained by

$$F_{ground} = I/\tilde{I}, \tag{2}$$

where F_{ground}=0 . . . 1.2. The cloud modification factor can become greater than 1 (upper limit 1.2) because for clouds nearby the position of the sun the radiation passing

through the atmosphere can be reflected at a cloud border thereby enhancing the radiation reaching the detector. In that case the measured value is greater than the clear sky model value. The enhancement of the measured value is allowed to become up to 20% of the model calculation result. For higher discrepancies a problem during the measurement is assumed and the data is discarded. The accuracy of the results of Eq. (2) is dependent on how representative the model calculations are for each site. This depends on the model used and on the chosen input parameters.

FastRT is a fast simulation tool for UV radiation developed by Ola Engelsen. Surface UV irradiances are obtained by interpolation in lookup tables of transmittances and reflectances. The lookup tables are computed using the accurate libRadtran atmospheric radiative transfer software package (Mayer and Kylling, 2005) with a couple of predefined input parameters. The agreement of both models when comparing calculated UV-Indexes for cloudless but aerosol loaded atmospheric conditions is at the 3% level (Engelsen and Kylling, 2005). For the benefit of fast computational time FastRT is used although the set of variable input parameters is restricted. The input parameters are altitude, solar zenith angle, day of year, albedo, ozone (altitude dependent forecast from DWD) and Ångström coefficient beta (Ångström coefficient alpha=1.3 predefined). Albedo and Ångström coefficient beta are dependent on altitude and on the snow line. To obtain suitable clear sky model results for each measurement site reasonable parameters are chosen. To check measured and modelled UV-Index for consistency, measurements performed at clear sky conditions have to be identified. This is done by using the cloud modification factors of the satellite images. A cloud modification factor larger than 0.98 at a site pixel indicates clear sky conditions for the given time. Using two years of measured data fulfilling this criterion a mean value of 0.92 of the ratio measurement/model was found. So the modelled values are on average 8% higher than the measurements at all sites. Since no measurements of albedo and aerosols are available the estimated input parameters may lead to this offset. Moreover the timing is not perfectly synchronous. The maximum time delay between satellite image (every 15 min) and the center of the measurement interval (10 or 30 min) of the ground

based devices is ±7.5 min. The ratio measurement/model is also varying from day to day which indicates changing atmospheric conditions with time. To reduce the error in Eq. (2) that is caused by this inconsistency, every day clear sky measurements and model results are compared leading to a correction factor for the modelled values. If there are no clear sky measurements on a given day the default value of 0.92 is used to reduce the model results.

3.3 Correlation of ground based and satellite derived CMF

A comparison between cloud modification factors estimated from satellite images and calculated from ground based measurements is shown in Fig. 1. One low altitude site (Klagenfurt, 448 m a.s.l.) and one high mountain station (Hafelekar, 2275 m a.s.l.) are chosen exemplarily. All other sites show similar results. For Hafelekar (Klagenfurt) 5315 (4311) time matching (maximal time delay ±7.5 min) data points for all weather conditions have been found from April 2005 up to November 2007. The black line indicates perfect correlation. The correlation for Klagenfurt data is best for clear sky conditions (around [1,1]) and overcast sky (below [0.2, 0.2]) but overall the scattering is quite bad. For the high mountain station Hafelekar the results are even worse, which is partly due to the problem of snow detection from satellite images described above. For clear sky conditions and snow covered mountains ($F_{\text{ground}} \rightarrow 1$) satellite derived cloud modification factors (F_{MSG}) are often low indicating clouds instead of snow. Moreover the low resolution of satellite images is more critical when compared with single spot measurements in mountainous regions (Hafelekar) than in flat country (Klagenfurt). Since these results are not satisfying correction methods had to be developed.

3.4 Correction of satellite derived cloud modification factors

For the final calculation of the UV-Index map area-wide cloud modification factors are needed, so the satellite estimates have to be corrected. Since the determination of cloud modification factors for snow covered satellite pixels is inaccurate, all CMF pixels

are split up in two groups with altitudes below and above the snow line. Unfortunately there is no data of the distribution of the snow line available in Austria. So the snow line altitude is estimated daily and assumed constant over the whole area. Based on the correlation of CMFs at the location of the ground site, a correction function is determined and spatially expanded to a region of 4° around the site with decreasing effect. Since the final UV-Index map covers the area from 46.25° up to 49.2° in latitude and from 9.3° up to 17.3° in longitude, all pixels lie within the correction range of at least one site pixel. There are different correction functions dependent on the correlation of CMFs at each site and dependent on the site altitude compared to the snow line.

Case 1: $F_{\text{ground}}>0.9$ and $F_{\text{MSG}}>0.9$ and altitude below the snow line: In this case there is a good correlation between both CMFs and the correction function $corr(F_{\text{MSG}})$ is the identity, see Fig. 2, Case 1. So the corrected CMF pixel $F^{\text{corr}}_{\text{MSG}}(x)$ is defined as

$$F^{\text{corr}}_{\text{MSG}}(x) = F_{\text{MSG}}(x) \tag{3}$$

with $x=0°...4°$.

Case 2: $F_{\text{ground}}>0.8$ and altitude above the snow line: There can be the problem of snow being detected as clouds in the vicinity of this site. This would lead to pixels with too low UV-Indexes. Since the final UV-Index maps are open to the public to inform about potential health risks, it is better to obtain bigger values for the UV-Index than lower ones. Therefore a correction function is implemented independent of the site pixel correlation of satellite derived and ground measured CMFs.

The correction function corr(F_{MSG}) is given by a straight line trough the points [$F_{\text{MSG}}, F_{\text{ground}}$] and [1, 1], see Fig. 2, Case 2. With this correction function all satellite determined CMFs with an altitude above the snow line are increased linearly with decreasing distance to the site pixel in the following way:

$$F^{\text{corr}}_{\text{MSG}}(x) = \text{corr}(F_{\text{MSG}}(x)) - \frac{x}{4}[\text{corr}(F_{\text{MSG}}(x)) - F_{\text{MSG}}(x)] \tag{4}$$

with $x=0°...4°$.

Case 3: Remaining correlations ($F_{\text{ground}} \leq 0.9$ and $F_{\text{MSG}} \leq 0.9$) with altitudes below the snow line and with altitude above the snow line ($F_{\text{ground}} \leq 0.8$): The correction function is a combination of two straight lines. The first one is starting at [0, 0] and ending at [F_{MSG}, F_{ground}] whereas the second one is from [F_{MSG}, F_{ground}] to [1, 1], see Fig. 2, Cases 3a and 3b. Again the correction is implemented as defined in Eq. (4) where the effect is decreasing with increasing distance. In this case the corrected CMF can be higher or lower than the satellite estimate taking into account situations with less or more clouds.

The correction methods described above strongly depend on the correlation of CMFs between satellite estimate and ground measurement at a single site. Since most CMF pixels are in between 4° of at least two site pixels, the distance weighted corrections gained from the two closest site pixels are finally used to calculate the corrected CMF value $\widehat{F}^{\text{corr}}_{\text{MSG}}(i)$ for pixel i, as defined in Eq. (5)

$$\widehat{F}^{\text{corr}}_{\text{MSG}}(i) = \frac{F^{\text{corr}}_{\text{MSG}}(x_1) \times x_2^2 + F^{\text{corr}}_{\text{MSG}}(x_2) \times x_1^2}{x_1^2 + x_2^2}. \tag{5}$$

The distances from pixel i to the two closest site pixels are denoted with x_1 and x_2. Because $F_{\text{ground}} \leq 1.2$ the correction can lead to $\widehat{F}^{\text{corr}}_{\text{MSG}} > 1$ in rare cases. So also $\widehat{F}^{\text{corr}}_{\text{MSG}}$ is limited to 1.2.

An example of the effect of the correction method can be seen in Fig. 3. First the cloud modification factor map estimated from satellite images that were obtained on 2 September 2007 at 16:30 UTC is shown (first row). In the second row the corrected CMF map is given and in the third row the difference of both maps can be seen. The snow line on this day was at an altitude of 2800 m a.s.l. which means that there was no snow except in the glacier regions. So all stations except the high mountain station Sonnblick were below the snow line. Measurements at Zugspitze and in Mariapfarr lead to a reduction in $\widehat{F}^{\text{corr}}_{\text{MSG}}$ whereas measurements in Innsbruck and at Hafelekar cause an enhancement. Moreover the decreasing effect of the correction with increasing distance can be seen nicely.

3.5 UV-Index map

In a final step the UV-Index map is calculated. Therefore a lookup table of clear sky UV-Indexes is computed with FastRt. The input parameters are altitudes in steps of 200 m from 0 to 4000 m, solar zenith angle, day of year, albedo, ozone (altitude dependent forecast from DWD) and Ångström coefficient beta. Albedo and Ångström coefficient beta are dependent on altitude and on the snow line. The solar zenith angle is calculated for the central pixel of the map at the time given by the satellite images. Next the corrected cloud modification factor map $\widehat{F}^{\mathrm{corr}}_{\mathrm{MSG}}$ is interpolated to the grid of the topography map with a resolution of approximately 1×1 km. Then for each pixel of the topography map the clear sky UV-Index is obtained from the lookup table. In the end the UV-Index map is generated by scaling the clear sky UV-Index with the corrected CMF for each pixel. The calculated UV-Index map for 12:45 local time on 16 August 2007 is shown in Fig. 4. The structure of the UV-Index which is indicated by predefined colors is caused by the satellite data derived cloud field and by topography. Based on new sets of satellite images every 15 min UV-Index maps are generated and available at http://www.uv-index.at/ with a time delay smaller than 30 min.

4 Conclusions

A method to generate UV-Index maps was presented by taking into account the main climatological parameters like clouds, ozone and aerosols. Cloud modification factors gathered from satellite images are corrected in the order of ±20% by means of ground based UV measurements. The correction methods based on the correlation of ground measured and satellite derived CMFs are empirically derived. In the case of snow cover in winter time the biggest discrepancies are found in the site pixel correlation. To overcome this problem of snow being detected as clouds in the derivation of CMFs from satellite data, corrections are applied that may lead to overvalue the actual UV-Index. As the data set of satellite images is expanding every day, more investigations

in the site pixel correlation of cloud modification factors are planned thereby improving the correction methods.

Acknowledgements. The Austrian UVB monitoring network is funded by the Austrian Federal Ministry of Agriculture, Forestry, Environment and Water Management. We thank all contributors for their supply of data to the Austrian UVB monitoring network.

References

Arola, A., Kalliskota, S., den Outer, P.N., Edvardsen, K., Hansen, G., Koskela, T., Martin, T.J., Matthijsen, J., Meerkoetter, R., Peeters, P., Seckmeyer, G., Simon, P.C., Slaper, H., Taalas, P. and Verdebout, J.: Assessment of four methods to estimate surface UV radiation using satellite data, by comparison with ground measurements from four stations in Europe, J. Geophys. Res., 107(D16), 4310, doi:10.1029/2001JD000462, 2002. 2149

Bais, A., Topaloglou, C., Kazadtzis, S., Blumthaler, M., Schreder, J., Schmalwieser, A., Henriques, D. and Janouch, M.: Report of the LAP/COST/WMO intercomparison of erythemal radiometers, World Meteorological Organization–Global Atmosphere Watch, Geneva, Switzerland, Rep. No. 141, 2000. 2147

Blumthaler, M.: Quality assurance and quality control methodologies within the Austrian UV monitoring network, Rad. Prot. Dos., 111, 4, 359–362, 2004. 2147

Engelsen O. and Kylling A.: Fast simulation tool for ultraviolet radiation at the Earth's surface, Opt. Eng., 44(4), 041012, doi:10.1117/12.639087, 2005. 2147, 2150

EUMETSAT: MSG Ground Segment LRIT/HRIT Mission Specific Implementation, EUM/MSG/SPE/057, 5, 2005. 2146

Krige, D. G.: Lognormal-de Wijsian Geostatistics for Ore Evaluation, South African Institute of Mining and Metallurgy Monograph Series, Geostatistics, 1, 51 pp., 1981. 2145

Leszczynski, K., Jokela, K., Ylianttila, L., Visuri, R. and Blumthaler, M.: Erythemally weighted radiometers in solar UV monitoring: results from MWO/STUK intercomparison, Photochem. Photobiol., 67, 212–221, 1998. 2147

Mayer, B. and Kylling, A.: Technical note: The libRadtran software package for radiative transfer calculations – description and examples of use, Atmos. Chem. Phys., 5, 1855–1877, 2005, http://www.atmos-chem-phys.net/5/1855/2005/. 2150

Schmalwieser, A. W. and Schauberger, G.: A monitoring network for erythemally-effective solar ultraviolet radiation in Austria: determination of the measuring sites and visualisation of the spatial distribution, Theor. Appl. Climatol., 69(3), 221–229, doi:10.1007/s007040170027, 2001. 2145

Verdebout, J.: A method to generate surface UV radiation maps over Europe using GOME, Meteosat, and ancillary geophysical data, J. Geophys. Res., 105(D4), 5049–5058, 2000. 2145, 2148

Verdebout, J.: A European satellite-derived UV climatology available for impact studies, Radiation Protection Dosimetry, 111, 4, 407–411, doi:10.1093/rpd/nch063, 2004. 2148

Verdebout, J. and Gröbner, J.: Mapping natural surface UV radiation with MSG: first maps and comparison with METEOSAT derived results and reference measurements, in: Proceedings of the EUMETSAT Meteorological Satellite Conference, Prague, Czech Republic, 31 May–4 June 2004, 558 pp., 2004 2149

World Health Organization: Global Solar UV Index: A Practical Guide, WHO, ISBN 92 4 159007 6, Geneva, 2002. 2147

Table 1. List of stations contributing to the Austrian UVB monitoring network.

Stations	Altitude [m a.s.l.]	Latitude [° N]	Longitude [° E]
Wien	153	48.26	16.43
Grossenzersdorf	156	48.20	16.57
Bad Vöslau	286	47.97	16.20
Steyregg/Linz	335	48.29	14.35
Graz	348	47.10	15.42
Dornbirn	410	47.43	9.73
Klagenfurt	448	46.65	14.32
München	530	48.15	11.57
Innsbruck	577	47.26	11.38
Mariapfarr	1153	47.15	13.75
Kanzelhöhe	1526	46.68	13.91
Davos	1610	46.80	9.83
Hafelekar	2275	47.32	11.39
Zugspitze	2660	47.42	10.98
Sonnblick	3106	47.05	12.96

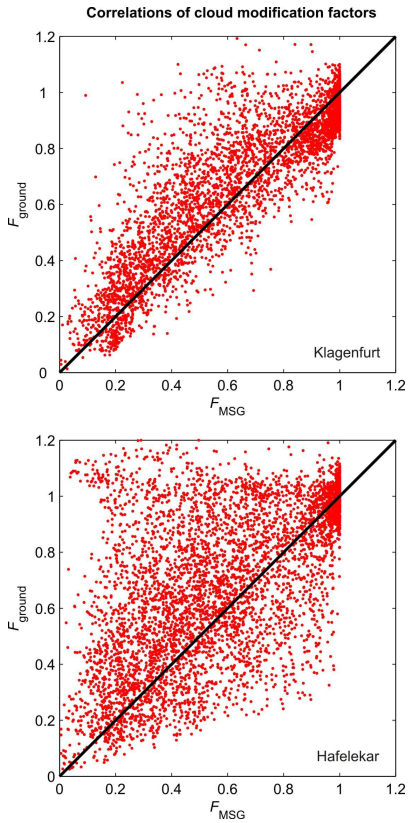

Fig. 1. Comparison of cloud modification factors estimated from satellite images (F_{MSG}) and obtained from ground based measurements (F_{ground}) for two sites (Klagenfurt and Hafelekar) of the Austrian UVB monitoring network. The black line indicates perfect correlation. All the data from April 2005 up to November 2007 is included which sums up to 4311 (5315) data points for Klagenfurt (Hafelekar) gathered on 543 (670) days in this period.

ACPD
8, 2143–2161, 2008

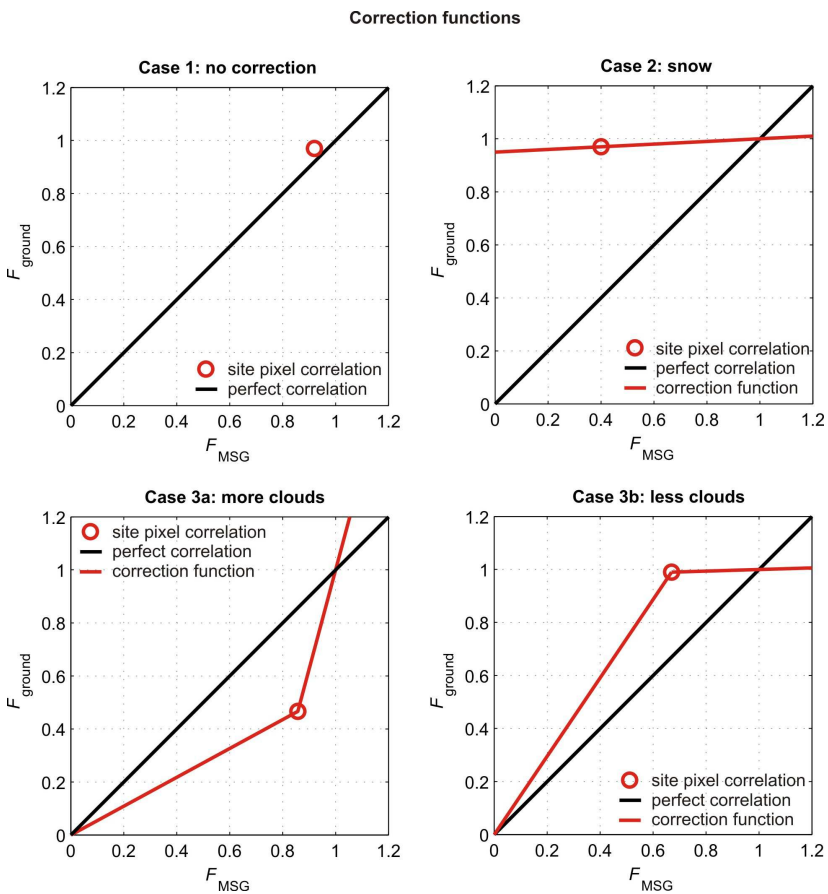

Fig. 2. Correction functions dependent on the site pixel correlation of CMFs and on the altitude in relation to the snow line as described in detail in Sect. 3.4.

ACPD
8, 2143–2161, 2008

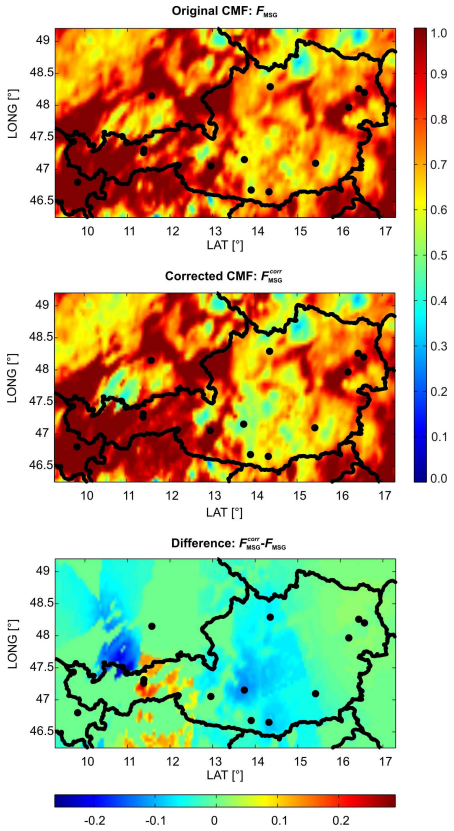

Fig. 3. Cloud modification factor map estimated from satellite images (first row) and cloud modification factor map corrected by means of ground based measurements (second row). The effect of the correction method is demonstrated as difference of both maps (third row), showing regions of enhancement and reduction in CMF. Black dots indicate the position of the ground based measurement sites of the Austrian UVB monitoring network.

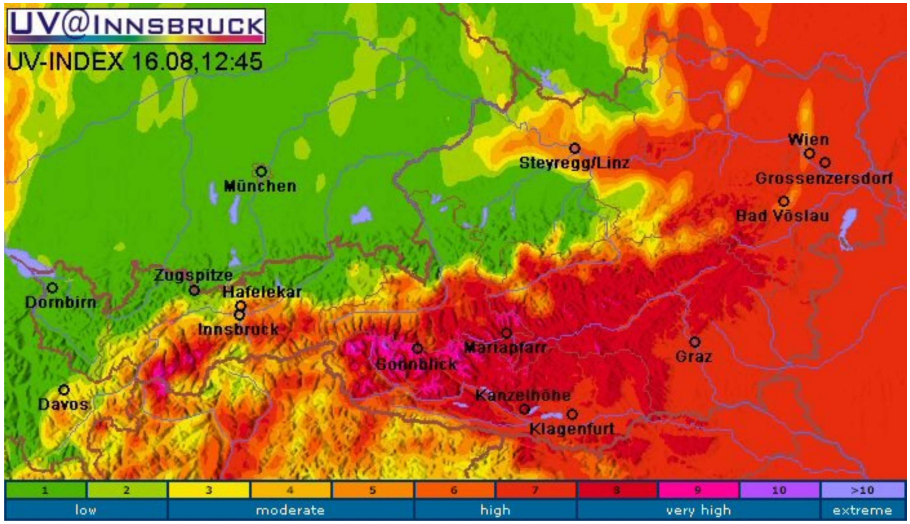

Fig. 4. UV-Index map generated by means of ground based UV measurements and cloud information derived from MSG satellite images on 16 August 2007 at 12:45 local time. The UV-Index is indicated by predefined colors.

ACPD
8, 2143–2161, 2008